Contribution of epigenetic mechanisms to variation in cancer risk among tissues

Michael Klutstein[a,1], Joshua Moss[b,c,1], Tommy Kaplan[c], and Howard Cedar[b,2]

[a]Laboratory for Research of Chromatin and Aging, Faculty of Dental Medicine, Institute of Dental Sciences, The Hebrew University of Jerusalem, Jerusalem, Israel 91120; [b]Department of Developmental Biology and Cancer Research, Institute for Medical Research Israel–Canada, Faculty of Medicine, The Hebrew University of Jerusalem, Ein Kerem, Jerusalem, Israel 91120; and [c]School of Computer Science and Engineering, The Hebrew University of Jerusalem, Jerusalem, Israel 91904

Edited by Stephen B. Baylin, Johns Hopkins University School of Medicine, Baltimore, MD, and accepted by Editorial Board Member Tak W. Mak January 21, 2017 (received for review October 6, 2016)

Recently, it was suggested that tissue variation in cancer risk originates from differences in the number of stem-cell divisions underlying each tissue, leading to different mutation loads. We show that this variation is also correlated with the degree of aberrant CpG island DNA methylation in normal cells. Methylation accumulates during aging in a subset of molecules, suggesting that the epigenetic landscape within a founder-cell population may contribute to tumor formation.

methylation | polycomb | aging

One of the riddles of cancer has always been the extreme variation in lifetime risk for different tissues of the body, which may extend over four orders of magnitude (1). Although it has been suggested that these differences might be explained on the basis of how each individual cell type responds to environmental or hereditary effects (2, 3), a recent report by Tomasetti and Vogelstein (1) indicated that this variation may actually be linked to the inherent developmental properties of each tissue type. Using data from the literature, these authors showed that there is a strong correlation between lifetime cancer risk and the cumulative number of previous stem-cell divisions within each tissue. Their interpretation of these findings is that every round of DNA replication is associated with a constant error rate, leading to the random accumulation of somatic mutations, thereby increasing the chances of tumor formation. It is likely that many mutations also are caused by extrinsic factors (4). In any event, the more stem-cell divisions involved in tissue formation, the higher is the probability for cancer-causing mutations.

More than 10 years ago, it was proposed that epigenetic, as opposed to genetic, alterations may predispose to tumors, and these modifications represent a crucial target for cancer risk assessment (5). Indeed, an accumulating body of evidence suggests that cancer is characterized by many epigenetic changes in histone modification and DNA methylation that may influence tumor biology (6). Although some alterations in DNA methylation are of a tissue-specific nature, most occur in a global manner, with large regions of lamin-associated sequences becoming hypomethylated (7), whereas polycomb-bound CpG islands specifically undergo de novo modification (8–10). This pattern appears to involve a similar set of sites in all tumors but varies quantitatively between different cell types (11). Furthermore, as opposed to some methylation events that take place after tumor formation, the abnormal CpG island modification profile can already be observed to some degree in normal tissues where it probably develops as a function of aging (11, 12), upstream to tumor transformation.

Results and Discussion

The fact that abnormal CpG island methylation varies with cell type prompted us to ask whether this epigenetic mark may have some bearing on the lifetime risk of cancer. To this end, we collected extensive DNA methylation data in normal human tissues from a large number of individuals of different ages, all extracted from The Cancer Genome Atlas (TCGA) and Gene Expression Omnibus (GEO) databases (Illumina 450K platform) by using fixed inclusion criteria (*Materials and Methods*) to guarantee fair representation. These unprocessed data were then corrected by applying a uniform background subtraction technique. To quantify the overall level of abnormal de novo methylation, we calculated the average β value for a defined set (n = 500) of polycomb-bound CpG islands known to carry the highest levels of aberrant methylation (*Materials and Methods*). For each tissue, data were compiled as a function of age (Fig. S1) extrapolated to 70 y to yield a single value and plotted against the lifetime risk of cancer. As seen in Fig. 1, there is a strong correlation ($P = 0.0006$) between these two variables, with a Pearson correlation (R) of 0.75, suggesting that up to 56% (R^2) of the variation in cancer risk may be attributed to tissue differences in abnormal methylation.

It should be noted that this correlation appears to be quite robust. These results, for example, were found to remain highly significant when the number of polycomb islands used for determining the level of aberrant methylation in each tissue was varied over a relatively wide range (Fig. S2). Although these data for high polycomb-bound islands were derived from the relatively neutral ES cell type, selection of islands from other specific cell types yielded similar results, consistent with the observation that these sites overlap between tissues (ref. 11; Fig. S2*C*). The relationship between aberrant methylation and lifetime risk of cancer was also found to be significant over a wide range of age choices and different combinations of test tissues (Fig. S3 *A* and *B*).

Significance

It is well-known that the risk of cancer varies widely between different tissues of the body with some cell types (e.g., colon, breast) being prone to cancer, whereas others (e.g., brain, bone) only rarely develop tumors, but the mechanism of this phenomenon has not been elucidated. Recently, it was shown that this risk coefficient may actually be related to the inherent number of stem-cell divisions that go into generating each individual cell type during development. In this work, we demonstrate that cancer risk is highly correlated with the degree of aberrant age-dependent methylation in normal tissues, clearly supporting the idea that cell-type tumor susceptibility may be influenced by biologically intrinsic epigenetic factors.

Author contributions: M.K., J.M., and H.C. designed research; M.K., J.M., T.K., and H.C. analyzed data; and M.K., J.M., and H.C. wrote the paper.

The authors declare no conflict of interest.

This article is a PNAS Direct Submission. S.B.B. is a Guest Editor invited by the Editorial Board.

Freely available online through the PNAS open access option.

[1]M.K. and J.M. contributed equally to this work.

[2]To whom correspondence should be addressed. Email: cedar@mail.huji.ac.il.

This article contains supporting information online at www.pnas.org/lookup/suppl/doi:10.1073/pnas.1616556114/-/DCSupplemental.

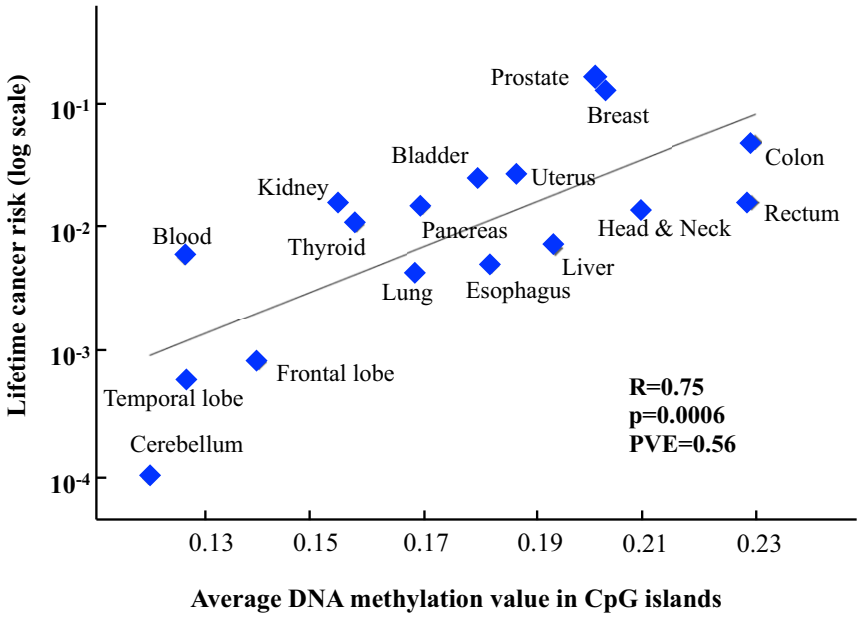

Fig. 1. Correlation between cancer lifetime risk and tissue DNA methylation. Methylation β-value scores were calculated from patient samples (n = 803) by using the Illumina 450K methylation array platform. The average methylation score at 500 polycomb-bound CpG islands was calculated, and normalized for each patient age, resulting in an estimated average methylation value at 70 y of age for each tissue (Fig. S1 and *Materials and Methods*). This value was plotted against cancer lifetime risk (in log scale), as calculated for each tissue (*Materials and Methods*), resulting in a Pearson correlation coefficient of 0.75 (P = 0.0006), and a Spearman correlation of 0.70 (P = 0.002) with the percentage of variance (PVE) being 0.56. It should be noted that the calculation of β value is a close approximation of percent methylation (36).

Intriguingly, the strongest correlation between DNA methylation and lifetime cancer risk, $R = 0.8$ ($P < 0.0001$) was found around age 50 with as few as 80 test CpG islands. Finally, we also demonstrated using bootstrapping (1,000 reiterations) that this correlation is robust and does not depend on the specific individual methylation samples used for each tissue type, with ~99% of the runs yielding a significant correlation ($P < 0.01$) (Fig. S3*C*).

It is well-known that abnormal de novo methylation takes place preferentially on CpG islands marked with the polycomb complex (8, 11, 13), but it is not clear what actually drives this modification. Mechanistically, this process probably involves the histone H3K27 methylase, EZH2, which has been shown to be capable of recruiting the DNA methylase machinery (14, 15). In this manner, these target CpG islands may slowly accumulate methyl groups that would then be faithfully maintained over long periods of time in normal tissues. One possibility is that abnormal methylation is linked to DNA replication, an idea that is in keeping with data showing that the level of CpG-island methylation in each tissue is closely correlated with the extent of stem-cell divisions contributing to this cell type (Fig. S4). A similar process appears to take place in tissue culture cell lines where this same profile of abnormal methylation increases with continued cell passage and replication (16). This idea would also explain why aberrant methylation increases as a function of aging, specifically in those tissues that are constantly being renewed through an adult stem-cell division process (Fig. S1). Although replication errors also increase with each division, the mechanism of aberrant DNA methylation probably operates in an independent manner through polycomb binding.

In light of this possibility, we next attempted to use statistical modeling to explore the relationships among aberrant DNA methylation, stem-cell division number, and lifetime risk of cancer. As a first step, we calculated how much of the methylation cannot be explained by stem-cell division number (Fig. S4*A*) (residual methylation), as well as the extent of lifetime risk that is not explained by the number of stem-cell divisions (Fig. S4*B*) (residual lifetime risk). A comparison of these residuals indicates that even after removing the influence of stem-cell divisions in each tissue, there is still a good correlation ($R = 0.74$, $P < 0.01$) between aberrant tissue methylation and lifetime risk of cancer (Fig. 2*A*). Conversely, when we first correlate lifetime risk with DNA methylation (Fig. 1, R = 0.75), thus explaining 56% of the variance [percentage of variance (PVE)], there is no significant correlation between the residual number of stem-cell divisions and residual lifetime cancer risk ($R = -0.03$, $P < 1$), (Fig. S4*C*). We then used linear regression analysis to model the influence of DNA methylation and stem-cell division number on the lifetime risk of cancer (Fig. 2*B*). DNA methylation alone was able to explain 77% of the variance, whereas the number of stem-cell divisions alone could only account for 49% of the variance in lifetime risk. A combined model considering both methylation and stem-cell divisions did not explain any more of the variance than methylation alone. It should be noted, however, that cancer risk must also depend on other factors, as well.

Considering the connection between DNA methylation and lifetime cancer risk, we next asked whether this aberrant modification is spread out over the entire cell population and, thus, provides a general predicator for cancer risk, or, alternatively, methylation may be restricted to select cells with their proportion in the cell population being associated with risk. Previous studies on individual islands in a few different tissues have already demonstrated that most molecules are largely unmethylated, with only a small percentage being highly modified, suggesting that this aberrant methylation may be restricted to a small number of cells (11). To examine whether this distribution is typical for all CpG islands, we collected data from the literature for a number of different normal-tissue DNA samples by using genome-wide Reduced Representation Bisulfite Sequencing (RRBS) to analyze the molecular distribution of DNA methylation. This high-throughput method produces small fragments (40–220 bp) that cover almost all (>90%) CpG islands

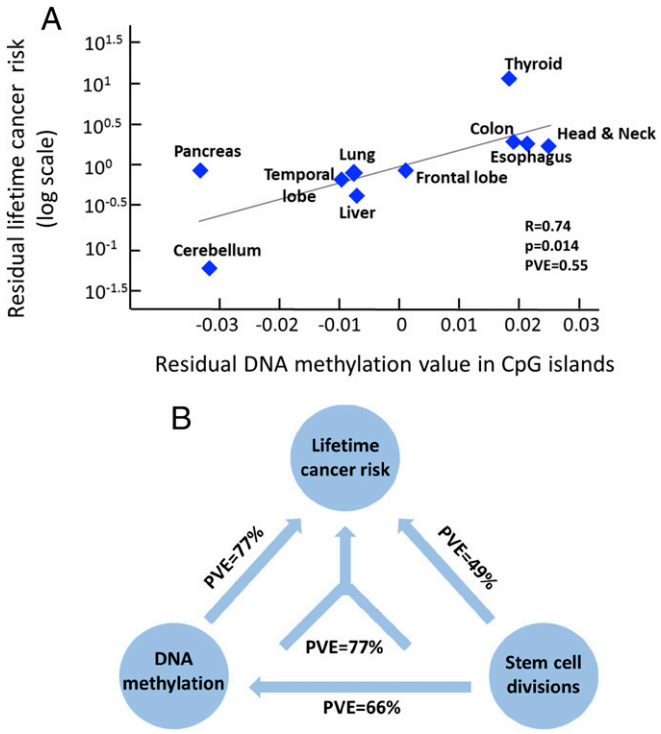

Fig. 2. Statistical modeling. (*A*) Residual cancer lifetime risk (i.e., effect not explained by stem-cell division number per tissue) vs. residual methylation (i.e., methylation not explained by correlation with stem-cell division number) as derived from the data in Fig. S4*A*. Here, we plot the 10 tissues for which all datasets were measured. This comparison is described by a Pearson correlation coefficient of 0.74 ($P = 0.014$). (*B*) Linear regression modeling of the statistical link among DNA methylation, cancer lifetime risk, and stem-cell divisions (*Materials and Methods*). Each arrow marks the percent of variance (PVE, *R*-squared) of the destination variable, explained by a linear model of the origin variable. For example, stem-cell division number explains 49% of the variance in cancer life time risk estimates over the different tissues (PVE = $R^2 = (0.7)^2$). The two-headed arrow signifies the cancer lifetime risk PVE given a multiple linear model of both DNA methylation and cell division number per tissue. *P* values calculated for each correlation: division vs. risk: $P = 0.024$; division vs. methylation: $P = 0.0045$; methylation vs. risk: $P = 0.0008$; divisions and methylation vs. risk: $P = 0.0057$. The PVE for DNA methylation vs. lifetime cancer risk (0.77) differs from that shown in Fig. 1 (0.56) because the analysis in Fig. 2 was based on the subset of tissues for which there is also data for cell division number (Table S1).

(17) in the genome including many molecules with strings of five CpG residues.

This molecule-by-molecule analysis indicated that polycomb-bound islands have a skewed distribution of methylation, with the number of molecules that are highly methylated (≥60%) being much greater than expected by chance (Fig. S5), and this same skewing was also seen in many different cell types (Table 1). In other words, DNA methylation in these tissues is not randomly distributed, but rather mostly concentrated in a relatively small number of molecules and although not yet confirmed by single cell analysis, these data strongly suggest that increased aberrant methylation may be indicative of more cancer-prone cells in the population.

Both abnormal demethylation, and CpG island-specific de novo methylation are characteristic of almost all types of cancer and have been implicated in tumor physiology with a high degree of DNA methylation being associated with poorer prognosis (18). In keeping with this picture, demethylation drugs, such as 5azaC, used either alone or in combination with other agents have been shown to be successful in treating many different cancer types (19–22), although the mechanism is unknown. In the mouse model for intestinal adenomas (min$^-$), it has been demonstrated that whereas this mutation may be necessary to initiate tumors, DNA methylation is essential for tumor growth (23), and the same may be true for other cancer types in mice (24). Furthermore, targeted methylation of the p16 (Ink4a) polycomb gene promoter leads to increased incidence of spontaneous tumors in mice (25). In some cases, it appears that aberrant demethylation may also play a role in tumorigenesis (26, 27). These observations suggest that both genetic and epigenetic changes play critical and parallel roles in tumor biology. Our findings serve to strengthen this basic idea by demonstrating that the chance of developing cancer in a particular tissue is highly correlated with the underlying level of abnormal de novo methylation in the same cell type even before tumorigenesis. It should be noted that the pattern of CpG-island methylation appears to be universal and similar in all cancer cell types (11), suggesting that this abnormal methylation constitutes a genuine epigenetic component independent of mutations.

The paper by Tomasetti and Vogelstein (1) nicely demonstrates that cancer risk is somehow correlated with the basic developmental design of each tissue as determined by counting the number of stem-cell divisions that go into its generation. It was further suggested that this elemental property has its effect by controlling the number of intrinsic mutations that each tissue accumulates and in this way influences cancer risk. Previous experiments have already demonstrated that normal cells accumulate aberrant methylation, perhaps as a function of aging (11, 12). Our studies, however, indicate that the amount of aberrant methylation that takes place in normal tissues is closely correlated with lifetime cancer risk, raising the possibility that this epigenetic change may also contribute to tumor susceptibility. Furthermore, statistical modeling of all of the data seem to imply that abnormal methylation itself may serve as a link that mediates the inherent association between stem-cell division number and cancer.

There is now considerable evidence demonstrating that abnormal methylation in normal tissues actually precedes the onset of tumors (11), and this early marker can be observed in individual crypts of the colon (28), in aging stem cells from the hematopoietic system (13) and in skin (29), raising the possibility that tumors themselves may evolve from normal cells that have already undergone excess de novo modification (30). In keeping with this idea, we have shown that tissue methylation is concentrated in a small number of individual CpG-island molecules, perhaps indicative of a fraction of cells that have undergone abnormal methylation (Table 1 and Fig. S5) (11). According to this idea, the risk of cancer in any given tissue would be correlated with the number of abnormally methylated precancer cells in that cell type. Because de novo modification appears to take place almost exclusively on CpG islands that are already silenced by polycomb in the normal tissue (8), we suggest that this modification works by preventing these genes from becoming activated, thereby inhibiting normal tissue differentiation, causing clonal selection for cells that may predispose to cancer (31).

Table 1. Molecular distribution of tissue DNA methylation

Tissue	Methylated reads	Expected reads	Fold enrichment
Breast	1,045	35	30
Lung	511	34	15
Liver	145	16	9
Prefrontal cortex	1,036	96	11
CD34$^+$ bone marrow cells	411	17	24

Calculation of fold enrichment for molecules having more than two of five CpG methylations using RRBS DNA methylation datasets (*Materials and Methods*) compared with the expected value as determined by its binomial distribution ($P < 10^{-300}$ for all samples) (Fig. S5).

Indeed, many of these methylation targets have been shown to be "driver" genes in a number of different cell types (Fig. S6).

Materials and Methods

Methylation Data. We included in our dataset samples from the TCGA and GEO databases for which DNA methylation profiles had been analyzed by using the Illumina Infinium HumanMethylation450 BeadChip Array, for which raw data were available, and the age of the sample donors. Data were retrieved from the following sources: For bladder, breast, colon, esophagus, head and neck, kidney, liver, lung, prostate, rectum, thyroid, and uterus, data were downloaded from the TCGA website: https://cancergenome.nih.gov. For blood, cerebellum, frontal lobe, temporal lobe (GSE43414), and pancreas (GSE49149), data were downloaded from the GEO database (www.ncbi.nlm.nih.gov/geo). It should be noted that some of these normal tissue samples were derived from cancer patients and may be slightly contaminated with tumor cells. Sample information is presented in Dataset S1.

Raw methylation data for all samples were processed by using the RnBeads software package (Max Planck Institute, rnbeads.mpi-inf.mpg.de/). The background fluorescence for each sample was estimated by means of negative control probes located on the array and used to normalize all samples to a reference sample, with the methylumi.lumi (Bioconductor) method (32). To measure the amount of aberrant methylation in each sample, we first identified the full set of CpG islands that are constitutively unmethylated in fetal tissues (11). For each CpG island, we calculated the mean H3K27me3 ChIP-seq occupancy in H1 ES cells (GSM537583) and selected 500 CpG islands with the highest levels of H3K27me3. This island set was then used to define the average methylation for each sample. We used robust linear regression (MASS R package) to compare the age and methylation for each sample and calculated the regressed methylation value for age 70. For Fig. S2*D*, where we varied the source tissue for H3K27me3 data, we have used the following dataset instead of H1 ES: H9 ES 2 (GSM706066), colon (GSM910564), brain (GSM772833), liver (GSM1112814), fetal brain (GSM621393), and fetal lung (GSM706852).

Lifetime Risk Values (by Tissue). Lifetime risk for the different cancer types was obtained from the following sources: The data for bladder (2.4%), colorectal (4.8%), esophagus (0.51%), kidney (1.61%), thyroid (1.08%), uterus (2.7%), and pancreas (1.49%) were obtained from the SEER data fact sheet (seer.cancer.gov/archive/csr/1975_2010/results_merged/topic_lifetime_risk.pdf). The data for breast (12.3%) and prostate (15%) were obtained from the American Cancer Society website (www.cancer.org). The data for head and neck (1.38%), liver (0.71%), lung (0.45%), and cerebellum (0.01%) were calculated by Vogelstein and Tomasetti (1). According to Cancer Research UK data (www.cancerresearchuk.org/health-professional/cancerstatistics/statistics-by-cancer-type/bowel-cancer/incidence#heading-Zero), the lifetime risk for rectal cancer is one-third that of colorectal cancer (4.8%/3 = 1.6%). As calculated by Vogelstein and Tomasetti (1), lifetime risk of glioblastoma is 0.22%. Because frontal lobe tumors represent 40% of the samples (33), their lifetime risk would be 0.088%. Temporal lobe tumors represent 29% of the samples, yielding a lifetime risk of 0.064%.

Nucleated (white) blood cells are made up of 70% from myeloid and 30% from lymphoid progenitors (34). Myeloid progenitors give rise to AML (lifetime risk 0.41%) and CML (lifetime risk 0.17%), whereas lymphoid progenitors give rise to ALL (lifetime risk 0.13%) and CLL (lifetime risk 0.52%) (SEER data fact sheet, 3 seer.cancer.gov/archive/csr/1975_2010/results_merged/topic_lifetime_risk.pdf). Using this information, we calculate the lifetime risk of blood tumors to be 0.6% ($0.3 \times (0.41+0.17) + 0.7 \times (0.13+0.52)$). All of the data for lifetime risk and DNA methylation are presented in Table S1. It should be noted that although the correlation between cell division number and lifetime cancer risk appears to be linear with both factors in log scale (1), we chose to compare methylation to cancer risk in a log linear relationship, because this presentation maximizes the (linear) Pearson Correlation between the two factors. The data for stem-cell division number were derived from Tomasetti and Vogelstein (1).

Data Processing. To analyze the molecular distribution of methylation in polycomb-targeted CpG islands, we analyzed RRBS data from several tissues (Fig. S5 and Table 1). RRBS data were downloaded from the GEO database (GSM683761, GSM919982, GSM1463824, GSM683821, GSM1045532) and analyzed as follows: Raw sequenced reads were filtered by quality, trimmed from barcode contamination by using trimGalore (Babraham Bioinformatics), and then aligned to the genome (version hg19) by using bismark (35). We collected all reads overlapping the top 500 H3K27me3-marked CpG islands that include runs of at least five CpGs, and counted how many of the sites were methylated in that particular sequenced read. We then compared the observed frequency of methylated reads with the expected number of methylated CpGs calculated according to a randomly generated binomial distribution with the same total number of reads and overall average methylation by using a bootstrap version of the Kolmogorov–Smirnov goodness-of-fit test as implemented in the Matching package in R (Fig. S5). The ratio between the observed and expected methylation for each tissue is presented in Table 1. Four Bootstrapping analysis was performed by using 1,000 iterations. In each iteration, a random selection of the original samples from each tissue (Fig. S1), the same size as the original group, was taken with replacements, and the resulting methylation of each tissue was compared with lifetime risk for that same tissue as described above. Residuals analysis was performed in the following manner. Residual methylation was defined as the difference between the observed methylation of each tissue and the methylation level predicted as a function of stem-cell divisions based on the optimal (log-)linear regression model. Similarly, residual lifetime risk was defined as the difference between the observed lifetime risk for each tissue and the predicted lifetime risk as a function of stem-cell divisions. Model analysis was performed to evaluate the relative contribution of methylation and stem-cell division number to lifetime cancer risk. Univariate and multivariate linear models were fitted by using the "stats" package in R. The code for analysis is presented in Dataset S2.

ACKNOWLEDGMENTS. This research was supported by grants from the European Research Council, the Israel Cancer Research Fund, Rosetrees Foundation, Lew Sanders, and the Smart Family Foundation.

1. Tomasetti C, Vogelstein B (2015) Cancer etiology. Variation in cancer risk among tissues can be explained by the number of stem cell divisions. *Science* 347(6217):78–81.
2. Danaei G, Vander Hoorn S, Lopez AD, Murray CJ, Ezzati M; Comparative Risk Assessment collaborating group (Cancers) (2005) Causes of cancer in the world: Comparative risk assessment of nine behavioural and environmental risk factors. *Lancet* 366(9499):1784–1793.
3. Fearon ER (1997) Human cancer syndromes: Clues to the origin and nature of cancer. *Science* 278(5340):1043–1050.
4. Wu S, Powers S, Zhu W, Hannun YA (2016) Substantial contribution of extrinsic risk factors to cancer development. *Nature* 529(7584):43–47.
5. Feinberg AP, Ohlsson R, Henikoff S (2006) The epigenetic progenitor origin of human cancer. *Nat Rev Genet* 7(1):21–33.
6. Esteller M (2011) Epigenetic changes in cancer. *F1000 Biol Rep* 3:9.
7. Berman BP, et al. (2011) Regions of focal DNA hypermethylation and long-range hypomethylation in colorectal cancer coincide with nuclear lamina-associated domains. *Nat Genet* 44(1):40–46.
8. Schlesinger Y, et al. (2007) Polycomb-mediated methylation on Lys27 of histone H3 pre-marks genes for de novo methylation in cancer. *Nat Genet* 39(2):232–236.
9. Widschwendter M, et al. (2007) Epigenetic stem cell signature in cancer. *Nat Genet* 39(2):157–158.
10. Ohm JE, et al. (2007) A stem cell-like chromatin pattern may predispose tumor suppressor genes to DNA hypermethylation and heritable silencing. *Nat Genet* 39(2):237–242.
11. Nejman D, et al. (2014) Molecular rules governing de novo methylation in cancer. *Cancer Res* 74(5):1475–1483.
12. Maegawa S, et al. (2014) Age-related epigenetic drift in the pathogenesis of MDS and AML. *Genome Res* 24(4):580–591.
13. Sun D, et al. (2014) Epigenomic profiling of young and aged HSCs reveals concerted changes during aging that reinforce self-renewal. *Cell Stem Cell* 14(5):673–688.
14. Viré E, et al. (2006) The Polycomb group protein EZH2 directly controls DNA methylation. *Nature* 439(7078):871–874.
15. O'Hagan HM, et al. (2011) Oxidative damage targets complexes containing DNA methyltransferases, SIRT1, and polycomb members to promoter CpG Islands. *Cancer Cell* 20(5):606–619.
16. Weidner CI, et al. (2013) Hematopoietic stem and progenitor cells acquire distinct DNA-hypermethylation during in vitro culture. *Sci Rep* 3:3372.
17. Boyle P, et al. (2012) Gel-free multiplexed reduced representation bisulfite sequencing for large-scale DNA methylation profiling. *Genome Biol* 13(10):R92.
18. Tsai HC, et al. (2012) Transient low doses of DNA-demethylating agents exert durable antitumor effects on hematological and epithelial tumor cells. *Cancer Cell* 21(3):430–446.
19. Kantarjian H, et al. (2006) Decitabine improves patient outcomes in myelodysplastic syndromes: Results of a phase III randomized study. *Cancer* 106(8):1794–1803.
20. Juergens RA, et al. (2011) Combination epigenetic therapy has efficacy in patients with refractory advanced non-small cell lung cancer. *Cancer Discov* 1(7):598–607.
21. Nie J, Liu L, Li X, Han W (2014) Decitabine, a new star in epigenetic therapy: The clinical application and biological mechanism in solid tumors. *Cancer Lett* 354(1):12–20.

22. Li X, Mei Q, Nie J, Fu X, Han W (2015) Decitabine: A promising epi-immunotherapeutic agent in solid tumors. *Expert Rev Clin Immunol* 11(3):363–375.
23. Laird PW, et al. (1995) Suppression of intestinal neoplasia by DNA hypomethylation. *Cell* 81(2):197–205.
24. McCabe MT, et al. (2006) Inhibition of DNA methyltransferase activity prevents tumorigenesis in a mouse model of prostate cancer. *Cancer Res* 66(1):385–392.
25. Yu DH, et al. (2014) Targeted p16(Ink4a) epimutation causes tumorigenesis and reduces survival in mice. *J Clin Invest* 124(9):3708–3712.
26. Gaudet F, et al. (2003) Induction of tumors in mice by genomic hypomethylation. *Science* 300(5618):489–492.
27. Yamada Y, et al. (2005) Opposing effects of DNA hypomethylation on intestinal and liver carcinogenesis. *Proc Natl Acad Sci USA* 102(38):13580–13585.
28. Shibata D (2009) Inferring human stem cell behaviour from epigenetic drift. *J Pathol* 217(2):199–205.
29. Raddatz G, et al. (2013) Aging is associated with highly defined epigenetic changes in the human epidermis. *Epigenetics Chromatin* 6(1):36.
30. Klutstein M, Nejman D, Greenfield R, Cedar H (2016) DNA methylation in cancer and aging. *Cancer Res* 76(12):3446–3450.
31. Easwaran H, et al. (2012) A DNA hypermethylation module for the stem/progenitor cell signature of cancer. *Genome Res* 22(5):837–849.
32. Du P, Kibbe WA, Lin SM (2008) lumi: A pipeline for processing Illumina microarray. *Bioinformatics* 24(13):1547–1548.
33. Larjavaara S, et al. (2007) Incidence of gliomas by anatomic location. *Neuro-oncol* 9(3):319–325.
34. Alberts B, et al. (2002) *Molecular Biology of the Cell*, 4th Ed (Garland Science, New York).
35. Krueger F, Andrews SR (2011) Bismark: A flexible aligner and methylation caller for Bisulfite-Seq applications. *Bioinformatics* 27(11):1571–1572.
36. Bibikova M, et al. (2011) High density DNA methylation array with single CpG site resolution. *Genomics* 98(4):288–295.
37. Tamborero D, et al. (2013) Comprehensive identification of mutational cancer driver genes across 12 tumor types. *Sci Rep* 3:2650.